

LONG-TERM VARIABILITY IN THE LENGTH OF THE SOLAR CYCLE

MICHAEL L. ROGERS, MERCEDES T. RICHARDS

Department of Astronomy & Astrophysics, Penn State University, 525 Davey Laboratory, University Park, PA, 16802-6305

AND

DONALD ST. P. RICHARDS

Department of Statistics, Penn State University, 326 Thomas Building, University Park, PA, 16802-2111

astro-ph, 2006 June 27

ABSTRACT

Detailed models of the solar cycle require information about the starting time and rise time as well as the shape and amplitude of the cycle. However, none of these models includes a discussion of the variations in the length of the cycle, which has been known to vary from ~ 7 to 17 years. The focus of our study was to investigate whether this range was associated with a secular pattern in the length of the sunspot cycle. To provide a basis for the analysis of the long-term behavior of the Sun, we analyzed archival data of sunspot numbers from 1700 - 2005 and sunspot areas from 1874 - 2005. The independent techniques of power spectrum analysis and phase dispersion minimization were used to confirm the ~ 11 -year Schwabe Cycle, and to illustrate the large range in the length of this cycle. Long-term cycles were identified in archival data from 1610 - 2000 using median trace analyses of the length of the cycle, and from power spectrum analyses of the (O-C) residuals of the dates of sunspot minima and maxima. The median trace analysis suggested that the cycle length had a period of 183 - 243 years, while the more precise power spectrum analysis identified a period of 188 ± 38 years. We found that the 188-year cycle was consistent with the variation of sunspot numbers and seems to be related to the Schwabe Cycle. We found a correlation between the times of historic minima and the length of the sunspot cycle such that the length of the cycle was usually highest when the actual number of sunspots was lowest. The cycle length was growing during the Maunder Minimum when there were almost no sunspots visible on the Sun. This information can now be used to improve the accuracy of the current solar cycle models, to better predict the starting time of a given cycle.

Subject headings: stars: activity – stars: flare – stars: individual (Sun) – Sun: sunspots

1. INTRODUCTION

Solar Cycle 23 was predicted to reach a maximum in early 2000 (Joselyn et al. 1996), with severe geomagnetic storms expected between 1999 and 2005. However, this cycle had modest activity compared to the previous two cycles (e.g., de Toma et al. 2004). Our work was motivated by the publicity associated with this solar cycle because of the relatively high level of solar activity exhibited through flares in 2003 October and November. Balasubramaniam & Regan (1994) showed that the temporal behavior of solar flares was similar to a sunspot butterfly diagram, with a typical 11-year cycle. Our interest in predicting magnetic activity cycles associated with other cool stars (e.g., Richards, Waltman, Ghigo, & Richards 2003) led us to investigate the long-term behavior of the solar cycle. Earlier analyses of the sunspot cycle have been summarized by Kuklin (1976) and Hathaway & Wilson (2004), and a review of the long-term solar cycle was presented by Usoskin & Mursula (2003).

In 1843, Heinrich Schwabe reported that he had identified a possible 10-year periodicity in the pattern of sunspots based on his 17-year study of the Sun from 1826–1843 (Schwabe 1844). (Note the typographical

error in Wilson (1994) that the result was based on a 43-year study.) In 1848, Rudolph Wolf introduced the relative sunspot number (R) and organized a program of daily observations of sunspots. He reanalyzed all earlier data and found that the average length of a solar cycle was about 11 yrs. For more than two centuries, solar physicists have applied a variety of techniques to determine the nature of the solar cycle. The earliest methods involved counting sunspot numbers and determining durations of cyclic activity from sunspot minimum to minimum using the “smoothed monthly mean sunspot number” (Waldmeier 1961; Wilson 1987, 1994). The “Group sunspot number” introduced by Hoyt & Schatten (1998) is a better documented data set than the database of relative sunspot numbers, but the two data sets since 1882 are virtually identical (Hathaway & Wilson 2004).

Since 1874, sunspot areas have been measured in terms of the total surface area of the solar disk covered by sunspots at a given time (Hathaway 2004). The analysis of sunspot numbers or sunspot areas is often referred to as a one-dimensional approach because there is only one independent variable, namely sunspot numbers or areas (Wilson 1994). Recently, Li et al. (2005) introduced a new parameter called the “sunspot unit area” in an effort to combine the information about the sunspot numbers and sunspot areas to derive the length of the cycle. There

is also a two-dimensional approach in which the latitude of an observed sunspot is introduced as a second independent variable (Wilson 1994). When sunspots first appear on the solar surface they tend to originate at latitudes around 40 degrees and migrate toward the solar equator. When such migrant activity is taken into account it can be shown that there is an overlap between successive cycles, since a new cycle begins while its predecessor is still decaying. This overlap became obvious when Maunder (1904) published his butterfly diagram and demonstrated the latitude drift of sunspots throughout the cycles. Maunder's butterfly diagram showed that although the length of time between sunspot minima is on average 11 years, successive cycles actually overlap by ~ 1 to 2 years. In addition, Wilson (1987) found that there were distinct solar cycles lasting 10 years as well as 12 years. This type of behavior suggests that there could be a cyclic pattern in the length of the sunspot cycle.

Sunspot number data collected prior to the 1700's show epochs in which there were almost no sunspots visible on the solar surface. One such epoch, known as the Maunder Minimum, occurred between the years 1642 and 1705, during which the number of sunspots recorded were very low in comparison to later epochs (Wilson 1994). Other studies include the analysis of geophysical data and tree-ring radiocarbon data, which contained residual traces of solar activity (Baliunas & Vaughan 1985), to determine if the Maunder period truly had a lower number of sunspots or whether it was simply a period in which little data were collected or large degrees of errors existed. While the data collected before the 1700's are typically less reliable than those collected in more recent times, the timing of the Maunder Minimum is still relatively accurate because of the correlation with geophysical data. Other epochs of minimum solar activity in the past have been noted, such as the Oort Minimum from 1010 - 1050, the Wolf Minimum from 1280 - 1340, the Spörer Minimum from 1420 - 1530 (Eddy 1977; Stuiver & Quay 1980; Siscoe 1980), and the Dalton Minimum from 1795 - 1823 (Soon & Yaskell 2003). These minima have been derived from historical sunspot records, auroral histories (Eddy 1976), and physical models linking dendrochronologically dated radiocarbon concentrations to the solar cycle (Solanki et al. 2004).

Currently, the fine details of a given solar cycle can be predicted accurately only after a cycle has begun (*e.g.*, Elling & Schwentek 1992; Hathaway, Wilson, & Reichmann 1994; and many others) because many solar cycle models require information about the starting time and rise time as well as the shape and amplitude of the cycle. Most of these models have focussed on the analysis of the International sunspot numbers of as many previous cycles as possible in order to predict the pattern for the current cycle. However, none of these models includes a discussion of the variations in the length of the cycle, which has been known to vary from ~ 7 to 17 years.

In this paper, we have investigated the variations in the length of the sunspot number cycle and examined whether the variability can be explained in terms of a secular pattern. Toward this goal, we applied classical one-dimensional techniques to rederive the periodicities of solar activity using the sunspot number and area data

TABLE 1
DURATION OF THE DATA

Data Set		Duration of Data
Spot Numbers	Daily	1818 Jan 8 - 2005 Jan 31
	Monthly	1749 Jan - 2005 Jan
	Yearly	1700 - 2004
Spot Areas	Daily	1874 May 9 - 2005 Feb 28
	Monthly	1874 May - 2005 Feb
	Yearly	1874 - 2004

to provide internal consistency in our analysis of the long-term behavior. These results were used as a basis in the study of the long-term behavior of the cycle length. In §2 we discussed the source of the data; in §3 we described the derivation of the cycle from sunspot numbers and sunspot areas using two independent techniques; in §4 we examined the variability in the cycle length based on the times of cycle minima and maxima using two independent techniques; and in §5 we discussed the results.

2. DATA COLLECTION

The sunspot data were collected from archival sources that catalog sunspot numbers, sunspot areas, as well as the measured length of the sunspot cycle. The sunspot number data, ranging from 1700 - 2005, were archived by the National Geophysical Data Center (NGDC). These data are listed in individual sets of daily, monthly, and yearly numbers. The relative sunspot number, R , is defined as $R = K(10g + s)$, where g is the number of sunspot groups, s is the total number of distinct spots, and the scale factor K (usually less than unity) depends on the observer and is "intended to effect the conversion to the scale originated by Wolf" (Coffey & Erwin 2004). The scale factor was 1 for the original Wolf sunspot number calculation. The spot number data sets are tabulated in Table 1 and plotted in Figure 1.

The sunspot area data, beginning in 1874 May 9, were compiled by the Royal Greenwich Observatory from a small network of observatories (Hathaway 2004). In 1976, the United States Air Force began compiling its own database from its Solar Optical Observing Network (SOON). The work continued with the help of the National Oceanic and Atmospheric Administration (NOAA) (Hathaway 2004). The NASA compilation of these separate data sets lists sunspot area as the total whole spot area in millionths of solar hemispheres. We have analyzed the compiled daily sunspot areas as well as their monthly and yearly sums. The sunspot area data sets were tabulated in Table 1 and plotted in Figure 2. Since the sunspot number and area data were collected in different ways and by different groups, there may be subtle inherent differences between the two data sets. However, these differences should reveal themselves when the data are analyzed.

The sunspot number cycle data were tabulated by the NGDC (Coffey & Erwin 2004) and are discussed further

TABLE 2
LENGTH OF THE SUNSPOT CYCLE

Year of Minimum	Year of Maximum	Cycle Length (from minima) (yr)	Cycle Length (from maxima) (yr)
1610.8	1615.5	8.2	10.5
1619.0	1626.0	15.0	13.5
1634.0	1639.5	11.0	9.5
1645.0	1649.0	10.0	11.0
1655.0	1660.0	11.0	15.0
1666.0	1675.0	13.5	10.0
1679.5	1685.0	10.0	8.0
1689.0	1693.0	8.5	12.5
1698.0	1705.5	14.0	12.7
1712.0	1718.2	11.5	9.3
1723.5	1727.5	10.5	11.2
1734.0	1738.7	11.0	11.6
1745.0	1750.3	10.2	11.2
1755.2	1761.5	11.3	8.2
1766.5	1769.7	9.0	8.7
1775.5	1778.4	9.2	9.7
1784.7	1788.1	13.6	17.1
1798.3	1805.2	12.3	11.2
1810.6	1816.4	12.7	13.5
1823.3	1829.9	10.6	7.3
1833.9	1837.2	9.6	10.9
1843.5	1848.1	12.5	12.0
1856.0	1860.1	11.2	10.5
1867.2	1870.6	11.7	13.3
1878.9	1883.9	10.7	10.2
1889.6	1894.1	12.1	12.9
1901.7	1907.0	11.9	10.6
1913.6	1917.6	10.0	10.8
1923.6	1928.4	10.2	9.0
1933.8	1937.4	10.4	10.1
1944.2	1947.5	10.1	10.4
1954.3	1957.9	10.6	11.0
1964.9	1968.9	11.6	11.0
1976.5	1979.9	10.3	9.7
1986.8	1989.6	9.7	10.7
1996.5 ¹	2000.3 ¹	—	—
Average		11.0±1.5	11.0±2.0

¹Predicted Cycle 23 values from NGDC (Coffey & Erwin 2004).

in §4. These data span dates from 1610 to 2000 (Table 2). Note that the final cycle length was derived from a predicted Cycle 23 minimum of 1996.5 and a predicted maximum of 2000.3.

3. THE LENGTH OF THE SUNSPOT CYCLE FROM SUNSPOT NUMBERS AND AREAS

The sunspot number and sunspot area data were analyzed to provide a basis for the analysis of the long-term

behavior of the Sun. We used the same techniques that were used by Richards, Waltman, Ghigo, & Richards (2003) in their study of radio flaring cycles of magnetically active close binary star systems.

3.1. Power Spectrum & PDM Analyses

Two independent methods were used to determine the solar activity cycles. In the first method, we analyzed the power spectrum obtained by calculating the Fast Fourier transform (FFT) of the data. The Fourier transform of a function $h(t)$ is described by $H(\nu) = \int h(t) e^{2\pi i \nu t} dt$ for frequency, ν , and time, t . This transform becomes a δ function at frequencies that correspond to true periodicities in the data, and subsequently the power spectrum will have a sharp peak at those frequencies. The Lomb-Scargle periodogram analysis for unevenly spaced data was used (Press et al. 1992).

In the second method, called the Phase Dispersion Minimization (PDM) technique (Stellingwerf 1978), a test period was chosen and checked to determine if it corresponded to a true periodicity in the data. The goodness of fit parameter, Θ , approaches zero when the test period is close to a true periodicity. PDM produces better results than the FFT in the case of non-sinusoidal data. The goodness of fit between a test period Π and a true period, P_{true} is given by the statistic, $\Theta = s^2/\sigma_t^2$ where, the data are divided into M groups or samples,

$$\sigma_t^2 = \frac{\sum(x_i - \bar{x})^2}{(N-1)}, \quad s^2 = \frac{\sum(n_j - 1)s_j^2}{(\sum n_j - M)},$$

s^2 is the variance of M samples within the data set, x_i is a data element (S_ν), \bar{x} is the mean of the data, N is the number of total data points, n_j is number of data points contained in the sample M , and s_j is the variance of the sample M . If $\Pi \neq P_{true}$, then $s^2 = \sigma_t^2$ and $\Theta = 1$. However, if $\Pi = P_{true}$, then $\Theta \rightarrow 0$ (or a local minimum).

All solutions from the two techniques were checked for numerical relationships with (i) the highest frequency of the data (corresponding to the data sampling interval), (ii) the lowest frequency of the data, dt (corresponding to the duration or time interval spanned by the data), (iii) the Nyquist frequency, $N/(2dt)$, and in the case of PDM solutions (iv) the maximum test period assumed. A maximum test period of 260 years was chosen for all data sets, except in the case of the more extensive yearly sunspot number data when a maximum of 350 years was assumed. We chose the same maximum test period for the sunspot area analysis for consistency with the sunspot number analysis, even though these test periods are longer than the duration of the area data.

3.2. Results of Power Spectrum and PDM Analyses

The results from the FFT and PDM analyses of sunspot number and sunspot area data are illustrated in Figures 3 and 4, corresponding to the daily, monthly, and yearly sunspot numbers and the daily, monthly, and yearly sunspot areas, respectively. In these figures, the top frame shows the power spectrum derived from the FFT analysis, while the bottom frame shows the Θ -statistic obtained from the PDM analysis. We specifically used two independent techniques so that we could

TABLE 3
SCHWABE SOLAR CYCLE DERIVED FROM FFT & PDM
ANALYSES

Data Set	Schwabe Cycle (yrs)		
	FFT	PDM	
Sunspot Numbers	daily	10.85 ± 0.60	10.86 ± 0.27
	monthly	11.01 ± 0.68	11.02 ± 0.68
	yearly	10.95 ± 0.72	11.01 ± 0.64
Average (Numbers)			10.95 ± 0.60
Sunspot Areas	daily	10.67 ± 0.44	10.67 ± 0.42
	monthly	10.67 ± 0.39	10.66 ± 0.39
	yearly	10.62 ± 0.39	10.62 ± 0.36
Average (Areas)			10.65 ± 0.40
Average (All data)			10.80 ± 0.50

test for consistency and determine the common patterns evident in the data. The fact that the two techniques produced similar results shows that the assumptions made in these techniques have minimal influence on the results. As expected, our results confirmed the work done by earlier studies.

The sunspot cycles derived from these results are summarized in Table 3. The most significant periodicities corresponding to the 50 highest powers and the 50 lowest θ values suggest that the solar cycle derived from sunspot numbers is 10.95 ± 0.60 years, while the value derived from sunspot area is 10.65 ± 0.40 years. The average sunspot cycle from both the number and area data is 10.80 ± 0.50 years. The strongest peaks in Figures 3 and 4 correspond to this dominant average periodicity over a range from ~ 7 years up to ~ 12 years. A weaker periodicity was also identified from the PDM analysis with an average period of 21.90 ± 0.66 years over a range from $\sim 20 - 24$ years.

The errors for the FFT and PDM analyses were derived by measuring the Full Width at Half Maximum (FWHM) of each dominant peak for each data set. The 1σ error is then defined by $\sigma = \text{FWHM}/2.35$. The three averages given in Table 3 were determined by averaging the dominant solutions from the FFT and PDM analyses for each data set. The errors in the averages were determined using standard techniques (Bevington 1969; Topping 1972). While the errors for the sunspot area results are smaller than those for the spot numbers, the area data are actually less accurate than the sunspot number data because the measurement error in the areas may be as high as 30% (Hathaway 2004). The higher errors for the area data are related to the difficulty in determining a precise spot boundary.

Longer periodicities that could not be eliminated because of relationships with the duration of the data set or other frequencies related to the data (as described in §3.1), were also identified with durations ranging from $\sim 90 - 260$ years (Figures 3 and 4). These long-term periodicities are discussed further in the following section.

4. VARIABILITY IN THE LENGTH OF THE SUNSPOT CYCLE FROM CYCLE MINIMA AND MAXIMA

The previous analysis of sunspot data provided some evidence of long term cycles in the sunspot data. This secular behavior was studied in greater detail through an analysis of the dates of sunspot minima and maxima from 1610 to 2000 tabulated by the NGDC (Coffey & Erwin 2004). Since there have been many concerns about the difficulty in deriving the exact times of minima, and the even greater complexity in the determination of sunspot maxima, we derived our results independently using the cycle minima as well as from the cycle maxima. The sunspot cycle lengths were derived by the NGDC from the dates of successive cycle minima. In addition, we have used their tabulated dates of cycle maxima to calculate the corresponding cycle lengths. These cycle lengths are tabulated in Table 2 and plotted in Figure 5. The data in Figure 5 show substantial variability over time.

The cycle lengths derived from the dates of sunspot minima and maxima were analyzed to search for periodicities in the cycle length using two techniques: (i) a median trace analysis and (ii) a power spectrum analysis of the 'Observed minus Calculated' or (O-C) residuals.

4.1. Median Trace Analysis

A median trace is a plot of the median value of the data contained within a bin of a chosen width, for all bins in the data set (Hoaglin et al. 1983). The median trace analysis depends on the choice of an optimal interval width (OIW). These OIWs, h_n , were calculated using three statistical methods based on theoretical arguments used routinely to estimate the statistical density function of the data. The first method defines the OIW as

$$h_{n,1} = \frac{3.49 \tilde{s}}{n^{1/3}} \quad (1)$$

where n is the number of data points and \tilde{s} , a statistically robust measure of the standard deviation of the data, is defined as

$$\tilde{s} = \frac{1}{n} \sum_{i=1}^n |x_i - M|, \quad (2)$$

where M is the sample median. The second method defines the OIW as

$$h_{n,2} = 1.66 \tilde{s} \left(\frac{\log_e n}{n} \right)^{1/3}. \quad (3)$$

A third definition of the OIW is given by

$$h_{n,3} = \frac{2 \times IQR}{n^{1/3}}, \quad (4)$$

where IQR is the interquartile range of the data set. Optimal bin widths were determined for three data sets corresponding to the cycle lengths derived from the (i) cycle minima, (ii) cycle maxima, and (iii) the combined minima and maxima data. Table 4 lists the solutions for the optimal interval widths ($h_{n,1}, h_{n,2}, h_{n,3}$) for each data set.

TABLE 4
OPTIMAL INTERVAL WIDTHS

Data Set	Data n	St. Dev. \tilde{s} (yrs)	Opt. Bin Width (yrs)		
			$h_{n,1}$	$h_{n,2}$	$h_{n,3}$
Cycle Minima	35	97.4	103.9	75.4	116.6
Cycle Maxima	35	97.0	103.4	75.1	115.4
Combined	70	97.3	82.4	63.5	91.8

Since the values of the optimal bin widths ranged from $\sim 60 - 120$ years, we tested the impact of different bin widths on our results. This procedure was limited by the fact that only 35 sunspot number cycles have elapsed since 1610 (see Table 2). The data set can be increased to 70 points if we analyze the combined values of the length of the solar cycle derived from both the sunspot minima and the sunspot maxima. Using our derived OIWs as a basis for our analysis, we calculated median traces for bin widths of 40, 50, 60, 70, 80, and 90 years. These are illustrated in Figure 6. The lower bin widths were included to make maximum use of the limited number of data points, and the higher bin widths were excluded because, once binned, there would be too few data points to make those analyses meaningful.

Figure 6 shows the binned data (median values) and the sinusoidal fits to the binned data. The Least Absolute Error Method (Bates & Watts 1988) was used to produce the sinusoidal fits to the median trace in each frame of the figure. These sinusoidal fits illustrate the long-term cyclic behavior in the length of the sunspot number cycle. The optimal solution was determined by identifying the fits that satisfied two criteria: (1) the cycle periods deduced from the three data sets should be nearly the same, and (2) the cyclic patterns should be in phase for the three data sets. Table 5 lists the derived cycle periods for all three data sets: the (a) cycle minima, (b) cycle maxima, and (c) combined minima and maxima data.

4.2. Results of Median Trace Analysis

The lengths of the sunspot number cycles tabulated by the National Geophysical Data Center (Table 2 & Figure 5) show that the basic sunspot number cycle is an average of (11.0 ± 1.5) years based on the cycle minima and (11.0 ± 2.0) years based on the cycle maxima. This Schwabe Cycle varies over a range from 8 to 15 years if the cycle lengths are derived from the time between successive minima, while the range increases to 7 to 17 years if the cycle lengths are derived from successive maxima. These variations may be significant even though the data in Figure 5 show *heteroskedasticity*, i.e., variability in the standard deviation of the data over time. Although the range in sunspot cycle durations is large, the cycle length converged to a mean of 11 years, especially after 1818 as the accuracy of the data became more reliable. In particular, the sunspot number cycle lengths from 1610 - 1750 show a wide range of variance while the cycle durations since 1818 show a much smaller variance (Figure 5). This variance may be influenced by the difficulty in

TABLE 5
DERIVED PERIODICITIES OF SUNSPOT NUMBER CYCLE

Bin Width (yrs)	Derived Periodicities (yrs)			
	Minima	Maxima	Both	Average
40	157	165	146	156 ± 10
50	185	182	182	183 ± 2
60	243	243	243	243
70	222	273	304	266 ± 41
80	393	349	419	387 ± 35
90	299	299	209	269 ± 52

identifying the dates of cycle minima and maxima whenever the sunspot activity is relatively low. Even after the data became more accurate there was still a significant ± 1.5 -year range about the 11-year mean. The range in the length of this cycle suggests that there may be a hidden longer-term variability in the Schwabe cycle.

Our median trace analysis of the lengths of the sunspot number cycle uncovered a long-term cycle with a duration between 146 and 419 years (Table 5), if the data are binned in groups of 40 to 90 years (see §4.1). Since the median trace analysis is influenced by the bin size of the data, we determined the optimal bin width based on the goodness of fit between the median trace and the corresponding sinusoidal fit (see Figure 6). Based on the sunspot minima (the best data set), the cycle length was 185 years for the 50-yr bin width, 243 years for the 60-yr bin, 222 years for the 70-yr bin, 393 years for the 80-year bin, and 299 years for the 90-yr bin; so we found no direct relationship between the bin size and the resulting periodicity. Figure 6 also shows the median traces for the data and illustrates that the optimal bin width is in the range of 50 - 60 years because it is only in these two cases that the sinusoidal fits are in phase and the derived periods are approximately equal for all three data sets. The 50-year median trace predicts a 183-year sunspot number cycle, while the 60-year trace predicts a 243-year cycle. Since the observations span ~ 385 years, there is greater confidence in the 183-year cycle than in the longer one because at least two cycles have elapsed since 1610. Similar long-term cycles ranging from 169 to 189 years have been proposed for several decades (Kuklin 1976).

4.3. Analysis of the (O-C) Data

The median trace analysis gives us a rough estimate of the long-term sunspot cycle. However, an alternative method to derive this secular period is to calculate the power spectrum of the (O-C) variation of the dates corresponding to the (i) cycle minima, (ii) cycle maxima, and (iii) the combined minima and maxima.

The following procedure was used to calculate the (O-C) residuals for each of the data sets given above, based only on the dates of minima and maxima listed in Table 2. First, we defined the cycle number, ϕ , to be $\phi = (t_i - t_0)/L$, where t_i are the individual dates of the extrema, and t_0 is the start date for each data set. Here, L is the

average cycle length (10.95 years) derived independently by the FFT and PDM analyses from the sunspot number data (§3.2). The (O-C) residuals were defined to be

$$(O - C) = (t_i - t_0) - (N_c \times L)$$

where, N_c is the integer part of ϕ and represents the whole number of cycles that have elapsed since the start date. The resulting (O-C) pattern was normalized by subtracting the linear trend in the data. This trend was found by fitting a least squares line to the (O-C) data. The normalized (O-C) data are shown in Figure 7 along with the corresponding power spectra.

4.4. Results of (O-C) Data Analysis

The power spectra of the (O-C) data in Figure 7 show that the long term variation in the sunspot number cycle has a dominant period of 188 ± 38 years. The Gleissberg cycle was also identified in this analysis, with a period of 87 ± 13 years. The solutions for these analyses are illustrated in Figure 7 and tabulated in Table 6. The 1σ errors were calculated from the FWHM of the power spectrum peaks, as described in §3.2. The sinusoidal fit to the (O-C) data in Figure 7 corresponds to the dominant periodicity of 188 years identified in the power spectra. Another cycle with a period of ~ 40 years was also found.

5. DISCUSSION AND CONCLUSIONS

The possible variability in the length of the sunspot cycle was examined through a study of archival sunspot data from 1610 – 2005. In the preliminary stage of our study, we analyzed archival data of sunspot numbers from 1700 - 2005 and sunspot areas from 1874 - 2005 using power spectrum analysis and phase dispersion minimization. This analysis showed that the Schwabe Cycle has a duration of (10.80 ± 0.50) years (Table 3) and that this cycle typically ranges from $\sim 10 - 12$ years even though the entire range is from $\sim 7 - 17$ years.

The focus of our study was to investigate whether this range was associated with a secular pattern in the length of the Schwabe cycle. We used our derived value for the Schwabe cycle from Table 3 to examine the long-term behavior of the cycle. This analysis was based on NGDC data from 1610–2000, a period of 386 years (using sunspot minima) or 385 years (using sunspot maxima). The long-term cycles were identified using median trace analyses of the length of the cycle and also from power spectrum analyses of the (O-C) residuals of the dates of sunspot minima and maxima. We used independent approaches because of the inherent uncertainties in deriving the exact times of minima and the even greater complexity in the determination of sunspot maxima. Moreover, we derived our results from both the cycle minima and the cycle maxima. The fact that we found similar results from the two data sets suggests that the methods used to determine these cycles (NGDC data) did not have any significant impact on our results.

The median trace analysis of the length of the sunspot number cycle provided secular periodicities of $183 - 243$ years. This range overlaps with the long-term cycles of

TABLE 6
DERIVED LONG TERM SOLAR CYCLES

Data Set	Gleissberg (yrs)	Secular (yrs)
Cycle Minima	86.8 ± 8.8	188 ± 40
Cycle Maxima	86.3 ± 18.1	187 ± 37
Combined	86.8 ± 10.7	188 ± 38
Average	86.6 ± 12.5	188 ± 38

$\sim 90 - 260$ years which were identified directly from the FFT and PDM analyses of the sunspot number and area data (Figures 3 and 4). The power spectrum analysis of the (O-C) residuals of the dates of minima and maxima provided much clearer evidence of dominant cycles with periods of 188 ± 38 years, 87 ± 13 years, and ~ 40 years. These results are significant because at least two long-term cycles have transpired over the ~ 385 -year duration of the data set.

The derived long-term cycles were compared in Figure 8 with documented epochs of significant declines in sunspot activity, like the Oort, Wolf, Spörer, Maunder, and Dalton Minima (Eddy 1977; Stuiver & Quay 1980; Siscoe 1980). In this figure, the modern sunspot number data were combined with earlier data from 1610-1715 (Eddy 1976) and with reconstructed (ancient) data spanning the past 11,000 years (Solanki et al. 2004). These reconstructed sunspot numbers were based on dendrochronologically-dated radiocarbon concentrations which were derived from models connecting the radiocarbon concentration with sunspot number (Solanki et al. 2004). The reconstructed sunspot numbers are consistent with the occurrences of the historical minima (e.g., Maunder Minimum). Solanki et al. (2004) found that over the past 70 years, the level of solar activity has been exceptionally strong. Our 188-year periodicity is similar to the 205-year de Vries-Seuss cycle which has been identified from studies of the carbon-14 record derived from tree rings (e.g., Wagner et al. 2001; Braun et al. 2005).

Figure 8 compares the historical and modern sunspot numbers with the derived secular cycles of length (a) 183 years (§4.2), (b) 243-years (§4.2), and (c) 188 years (§4.4). The first two periodicities were derived from the median trace analysis, while the third one was derived from the power spectrum analysis of the sunspot number cycle (O-C) residuals. The fits for the 183-year periodicity all had the same amplitude, but were moderately out of phase with each other, while the fits for the 243-year periodicity were perfectly in phase for all data sets, but with different amplitudes. This figure shows that the 183- and 188-year cycles provided a more consistent match to the sunspot number data than the 243-year cycle, especially during the Wolf, Spörer, Maunder, and Dalton Minima. In particular, we note that the more accurately determined 188-year cycle is consistent with the behavior of sunspot numbers over time. Moreover, the four historic minima since 1200, all occurred during the rising phase of our derived 188-year sunspot cycle when the length of the sunspot cycle was increasing. Figure 8

shows that, on average, the length of the sunspot cycle was highest when the actual number of sunspots was lowest. According to our model, the length of the sunspot cycle was growing during the Maunder Minimum when there were almost no sunspots visible.

The existence of long-term solar cycles with periods between 90 and 200 years is not new to the literature. However, the nature of these cycles is still not understood. While Hathaway (2004) noted evidence of a cycle of ~ 90 years in sunspot cycle amplitude variations, our studies of the length of the sunspot cycle have shown that the dominant cycle in these amplitude variations is 188 years, with weaker periods of ~ 40 and 87 years. Our results suggest that this 188-year cycle is related to the basic Schwabe Cycle. While we would like to confirm this result using a longer baseline (beyond 385 years), it should be noted that Schwabe's 10-year period was derived from only 17 years (less than two cycles) of observations (Schwabe 1844). In addition, it is well-known from Gauss' work on orbits that an orbit can be uniquely defined if at least three positions along that orbit are

known, as long as those positions cover critical parts of the orbit. So, our 188-year result may yet stand the test of time. Our model predicts that the length of the sunspot number cycle should increase gradually over the next ~ 75 years, accompanied by a gradual decrease in the number of sunspots. This information can now be used to improve the accuracy of the current solar cycle models (e.g., Dikpati, de Toma & Gilman 2006) to better predict the starting time of a given cycle.

We thank K. S. Balasubramaniam for his comments on the manuscript, Alon Retter for his comments on the research and for his advice on the (O-C) analysis, and David Heckman for advice on the data analysis. The SuperMongo plotting program (Lupton & Monger 1977) was used in this research. This work was partially supported by Penn State University, NSF grant AST-0074586, and an REU supplement to NSF grant AST-0434234 (PI - G.J. Babu) awarded to the Center for Astrostatistics at Penn State University.

REFERENCES

Balasubramaniam, K. S. & Regan, J. 1994, in Solar Active Region Evolution - Comparing Models with Observations, eds. K. S. Balasubramaniam & G. Simon, ASP Conference Series, 68, 17 (San Francisco: ASP)

Bevington, P. R. 1969, Data Reduction and Error Analysis for the Physical Sciences (New York: McGraw-Hill)

Baliunas, S. L., Vaughan, A. H. 1985, Ann. Rev. Astron. Astrophys., 23, 379

Bates, D. M. & Watts, D. G. 1988, Nonlinear Regression Analysis and Its Applications (New York: Wiley)

Braun, H., Christi, M., Rahmstorf, S., Ganopolski, A., Mangini, A., Kubatzki, C., Roth, K., & Kromer B. 2005, Nature, 438, 208

Coffey, H. E., and Erwin, E. 2004, National Geophysical Data Center, US Department of Commerce & National Oceanic and Atmospheric Administration, Boulder, CO, (<ftp://ftp.ngdc.noaa.gov>)

de Toma, G., White, O. R., Chapman, G. A., Walton, S. R., Preminger, D. G., & Cookson, A. M. 2004, ApJ, 609, 114

Dikpati, M., de Toma, G., & Gilman, P. 2006, Geophys. Research Lett., 33, 5102

Eddy, J. A. 1976, Science, Vol 192, p. 1189

Eddy, J. A. 1977, The Solar Output and Its Variation, ed. O.R. White, p. 51 (Boulder: Colorado Associated University Press)

Elling, W. & Schwentek, H. 1992, Solar Phys. 137, 155

Hathaway, D. H. 2004, Royal Greenwich Observatory/USAF/noaa, Sunspot Record 1874-2004, (<http://science.nasa.gov/ssl/pad/solar/greenwch.htm>)

NASA/Marshall Space Flight Center, Huntsville, AL

Hathaway, D.H., & Wilson, R.M. 2004, Solar Phys., 224, 5

Hathaway, D.H., Wilson, R.M., & Reichmann, E. 1994, Solar Phys., 151, 177

Hoaglin, D., Mosteller, F., & Tukey, J. 1983, Understanding Robust and Exploratory Data Analysis (New York: Wiley)

Hoyt, D. V. & Schatten, K. H. 1998, Solar Phys., 179, 189

Joselyn, J. A., Anderson, J., Coffey, H., Harvey, K., Hathaway, D., Heckman, G., Hildner, E., Mende, W., Schatten, K., Thompson, R., Thomson, A. W. P., & White, O. R. 1996, Solar Cycle 23 Project: Summary of Panel Findings (<http://www.sec.noaa.gov/info/Cycle23.html>)

Kuklin, G. V. 1976, Basic Mechanisms of Solar Activity, IAU Symp. No. 71, ed. V. Bumba, J. Kleczek, p. 47 (Boston: Reidel)

Li, K. J., Qiu, J., Su, T. W., & Gao, P.X. 2005, ApJ, 621, L81

Lupton, R., & Monger, P. 1977, The SuperMongo Reference Manual

Maunder, E. W. 1904, MNRAS, 64, 747

Press, W. H., Teukolsky, S. A., Vetterling, W. T., & Flannery, B. P. 1992, *Numerical Recipes in FORTRAN: The Art of Scientific Computing* (Cambridge: Cambridge University Press), 2nd edition.

Richards, M. T., Waltman, E. B., Ghigo, F., & Richards, D. St. P. 2003, ApJS, 147, 337

Schwabe, M. 1844, Astronomische Nachrichten, 21, 233

Siscoe, G. L. 1980, Rev. Geophys. Space Phys., 18, 647

Solanki, S. K., Usoskin, I.G., Kromer, B., SchüSSLer, M., & Beer, J. 2004, Nature, Vol. 431, No. 7012, p.1084

Soon, W., & Yaskell, S. H. 2003, Mercury, 32 (No.3), p. 13

Stellingwerf, R. F. 1978, AJ, 224, 953

Stuiver, M., & Quay, P. D. 1980, Science, 207, 11

Topping, J. 1972, Errors of Observation and Their Treatment (London: Chapman & Hall)

Usoskin, I. G., & Mursula, K. 2003, Solar Phys., 218, 319

Wagner, G., Beer, J., Masarik, J., Muscheler, R., Kubik, P., Mende, W., Laj, C., Raisbeck, G., & Yiou, F. 2001, Geophys. Research Lett., 28, 303

Waldmeier, M. 1961, The Sunspot Activity in the Years 1610-1960 (Zurich: Zurich Schulthess and Co. AG)

Wilson, P. R. 1994, Solar and Stellar Activity Cycles (New York: Cambridge University Press)

Wilson, R. M. 1987, J. Geophys. Res., 92, 10104

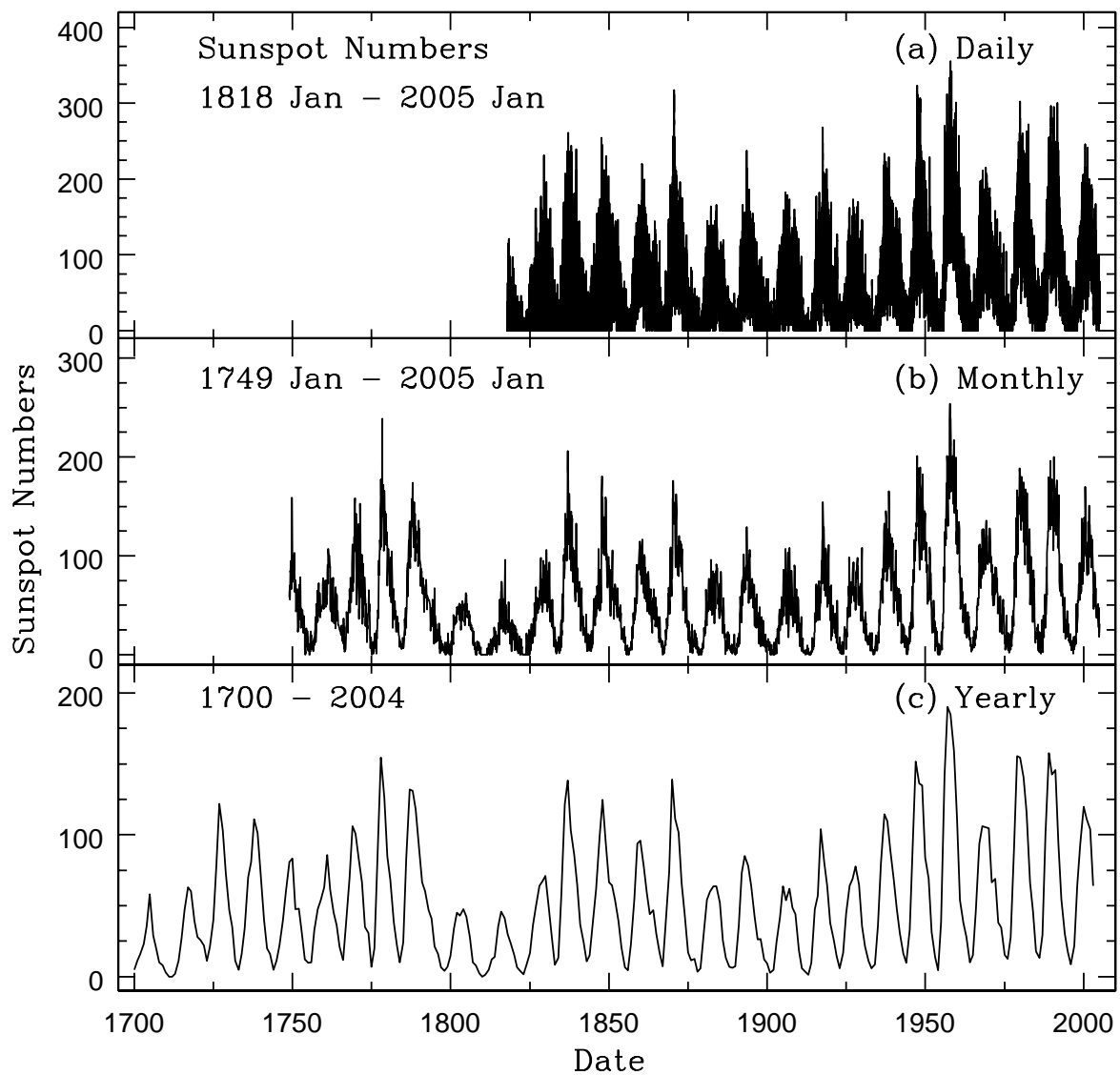


FIG. 1.— Archival data for (a) daily, (b) monthly, and (c) yearly sunspot numbers from 1700 to 2005.

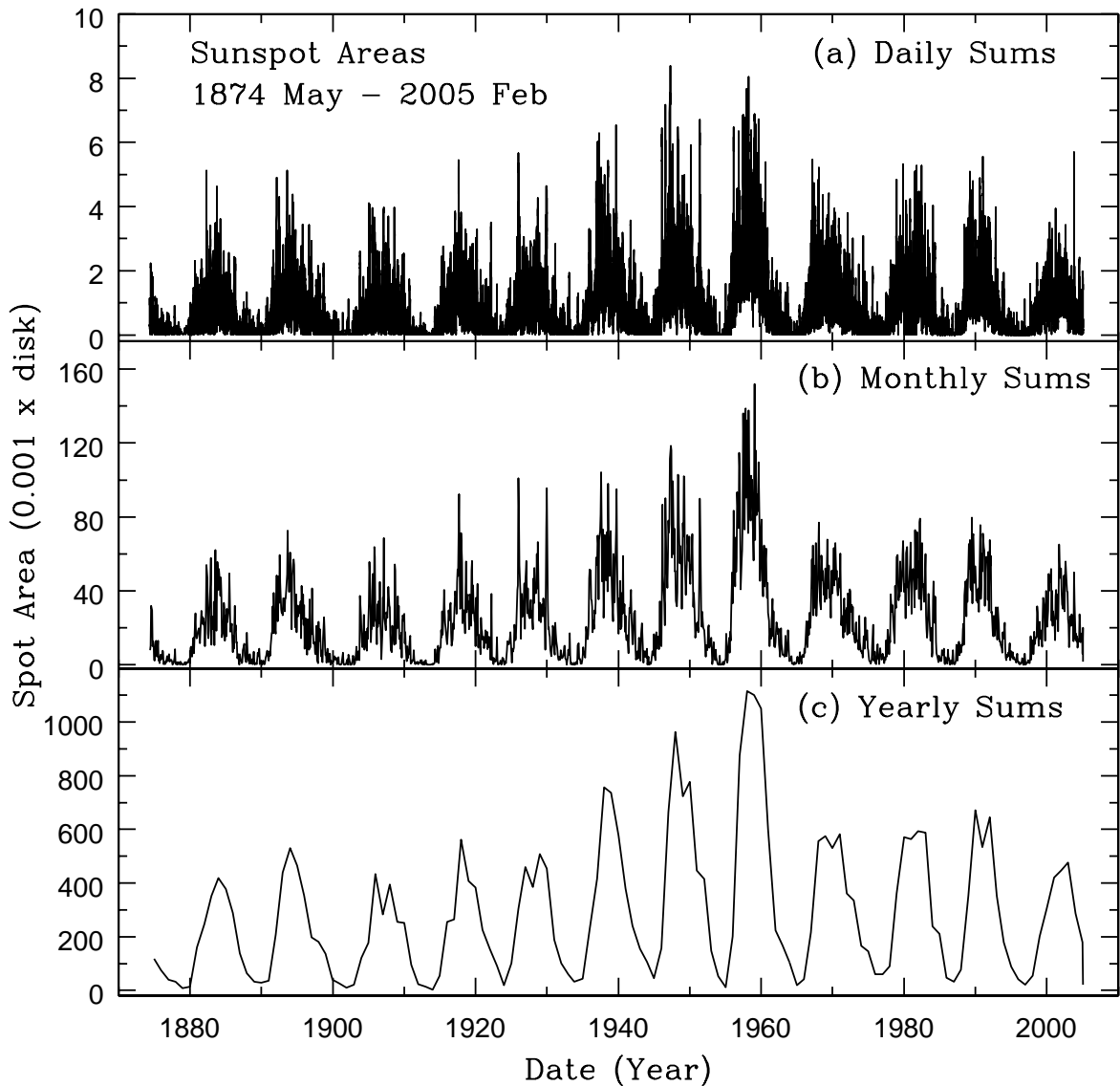


FIG. 2.— Archival data for (a) daily, (b) monthly, and (c) yearly sums of whole sunspot areas (0.001 x Solar Hemispheres) from 1874 May to 2005 February.

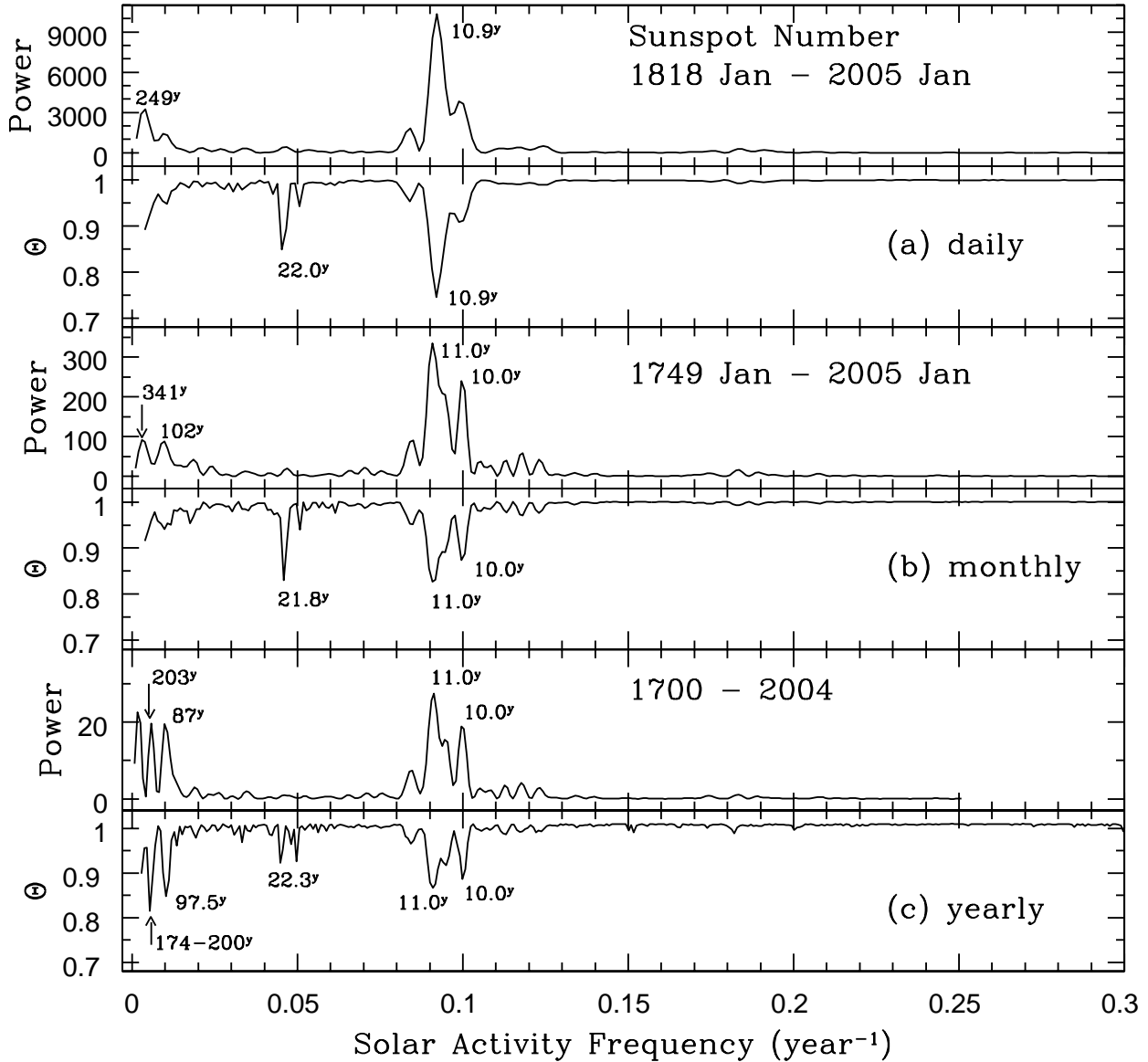


FIG. 3.— Frequencies of solar activity derived from power spectrum (upper frame) and PDM (lower frame) analyses calculated from (a) daily, (b) monthly, and (c) yearly sunspot numbers. The labels within the plot show the durations of the derived cycles in units of years.

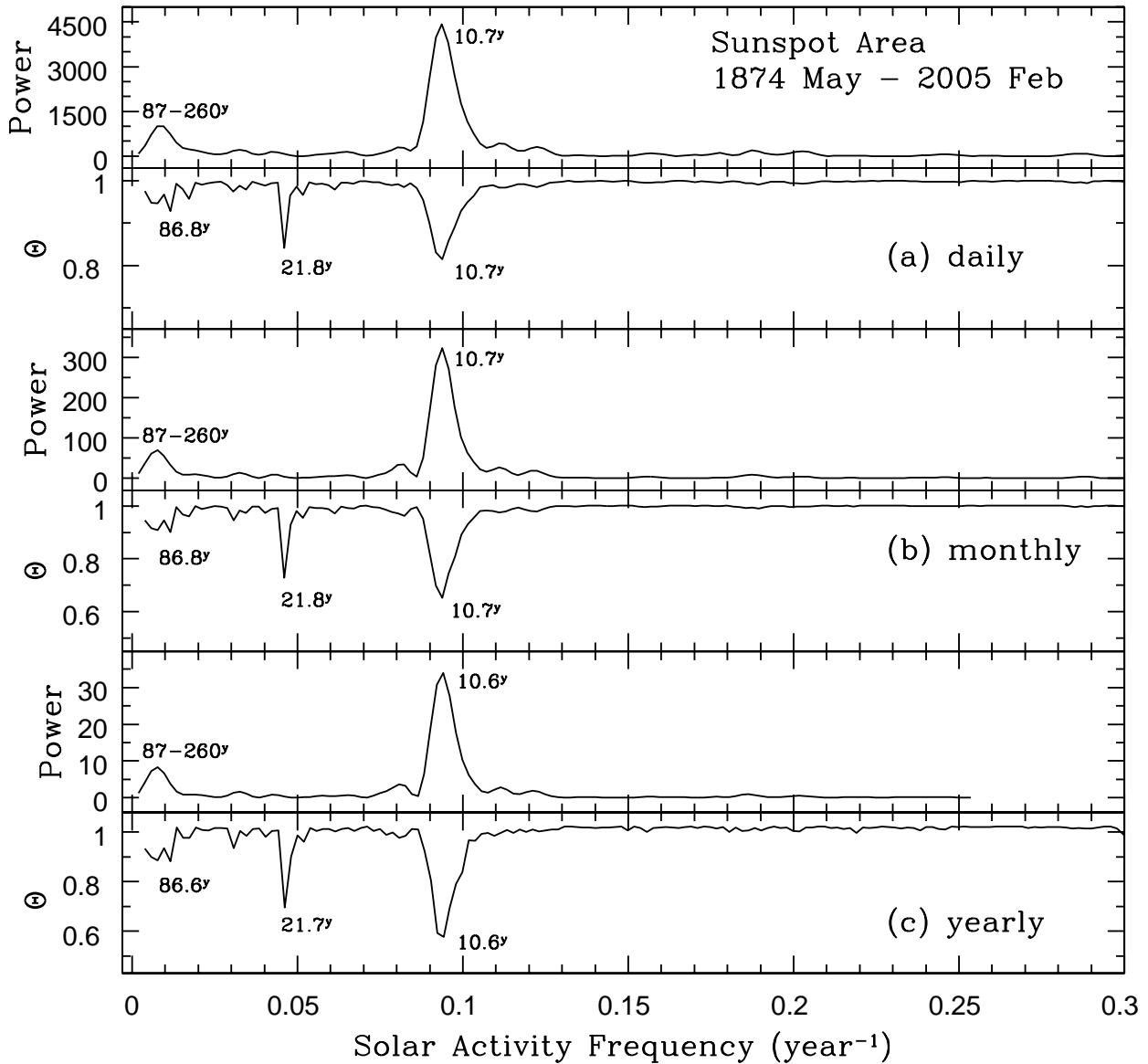


FIG. 4.— Frequencies of solar activity derived from power spectrum (upper frame) and PDM (lower frame) analyses calculated from (a) daily, (b) monthly, and (c) yearly sums of sunspot areas from 1874 May to 2005 February. The labels within the plot show the durations of the derived cycles in units of years.

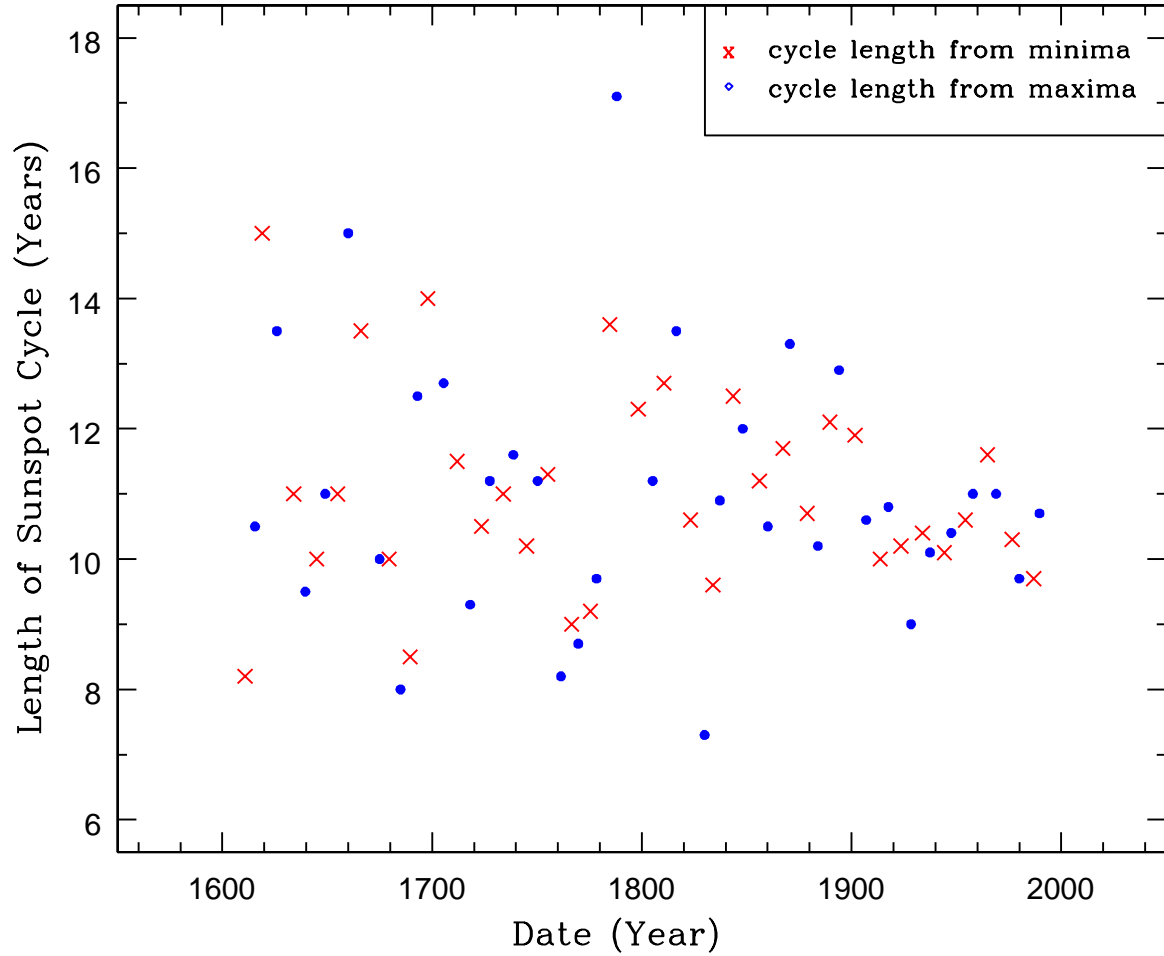


FIG. 5.— Sunspot cycle durations derived from successive minima (crosses) and successive maxima (dots) for dates from 1610.8 to 1989.6.

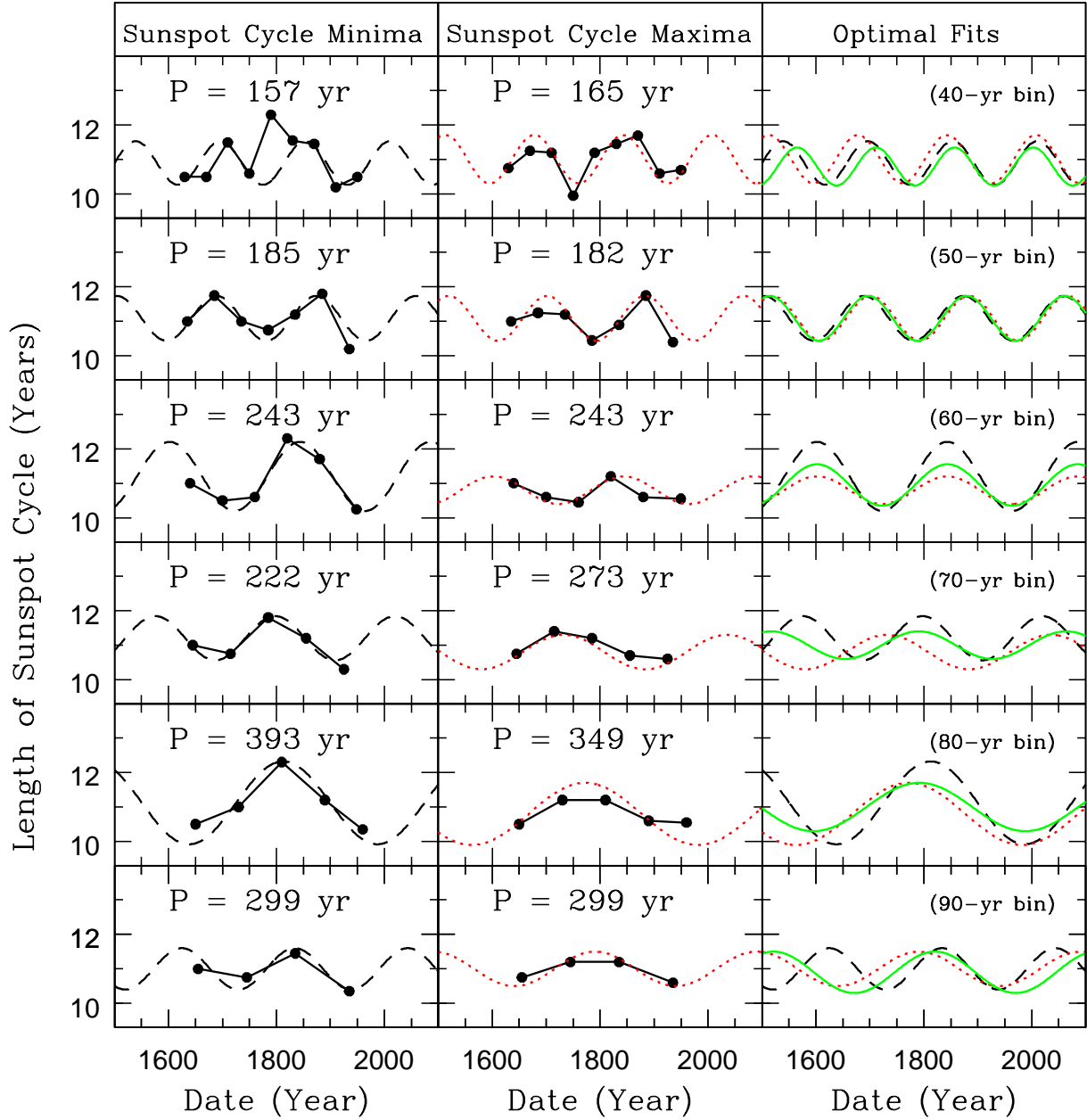


FIG. 6.— Median traces for sunspot minima (left column) and maxima (middle column) derived for bin widths of 40 – 90 years. A sinusoidal fit to the median trace is shown for each bin width (minima-dashed line, maxima-dotted line, and combined maxima and minima-solid line). The average period of each derived sinusoidal fit is given at the top of each frame. The optimal fits (right column) show that the optimal bin width is in the range of 50 – 60 years because it is only in these two cases that the sinusoidal fits are in phase and the derived periods are approximately equal for all three data sets.

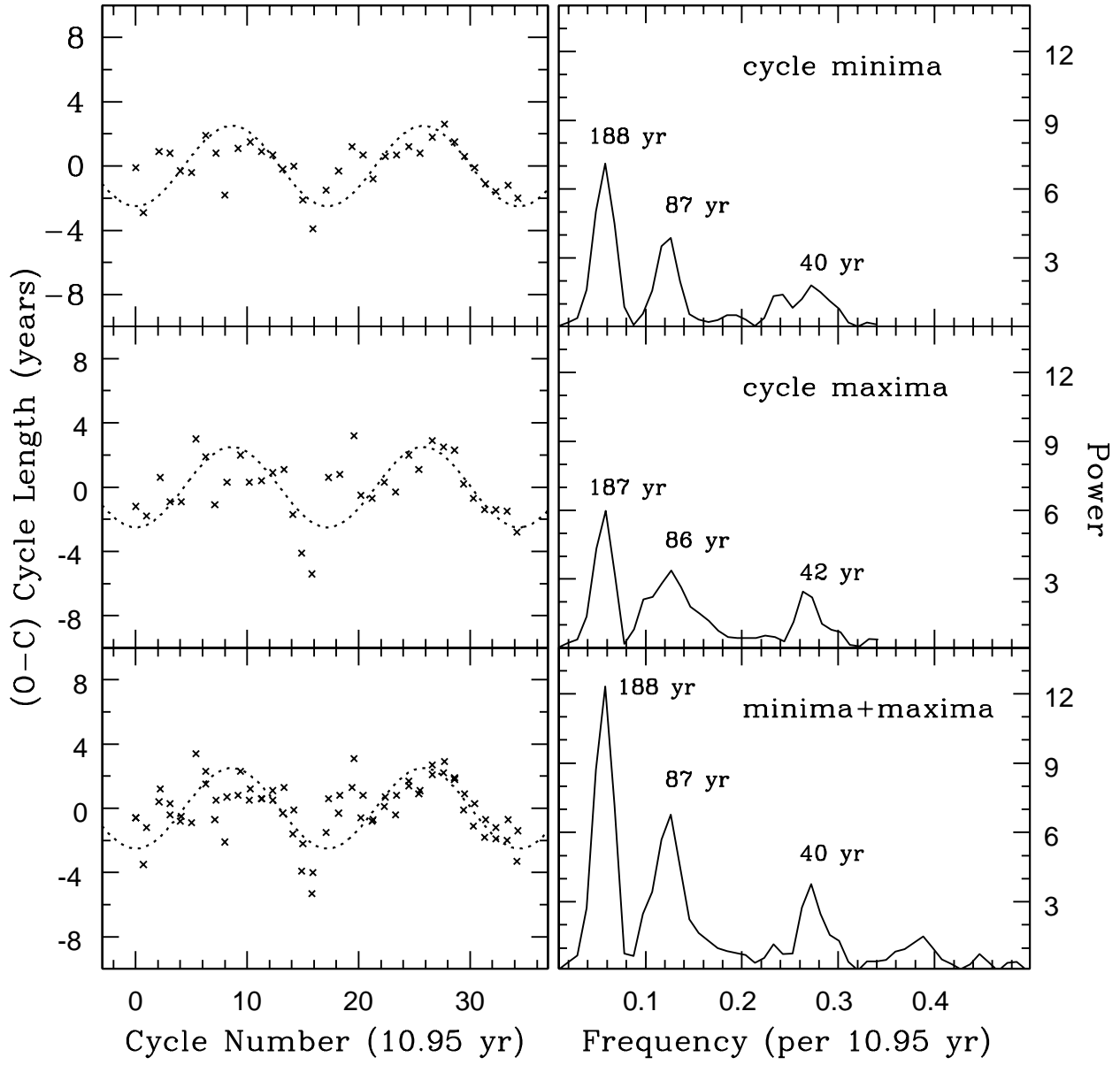


FIG. 7.— The cycle length ($O-C$) residuals (left frames) and the corresponding power spectrum (right frames) for the sunspot cycle minima (top frame), maxima (middle frame), and combined minima and maxima data (bottom frame). The dashed line through the data represents the long term cycle derived from the power spectrum analysis.

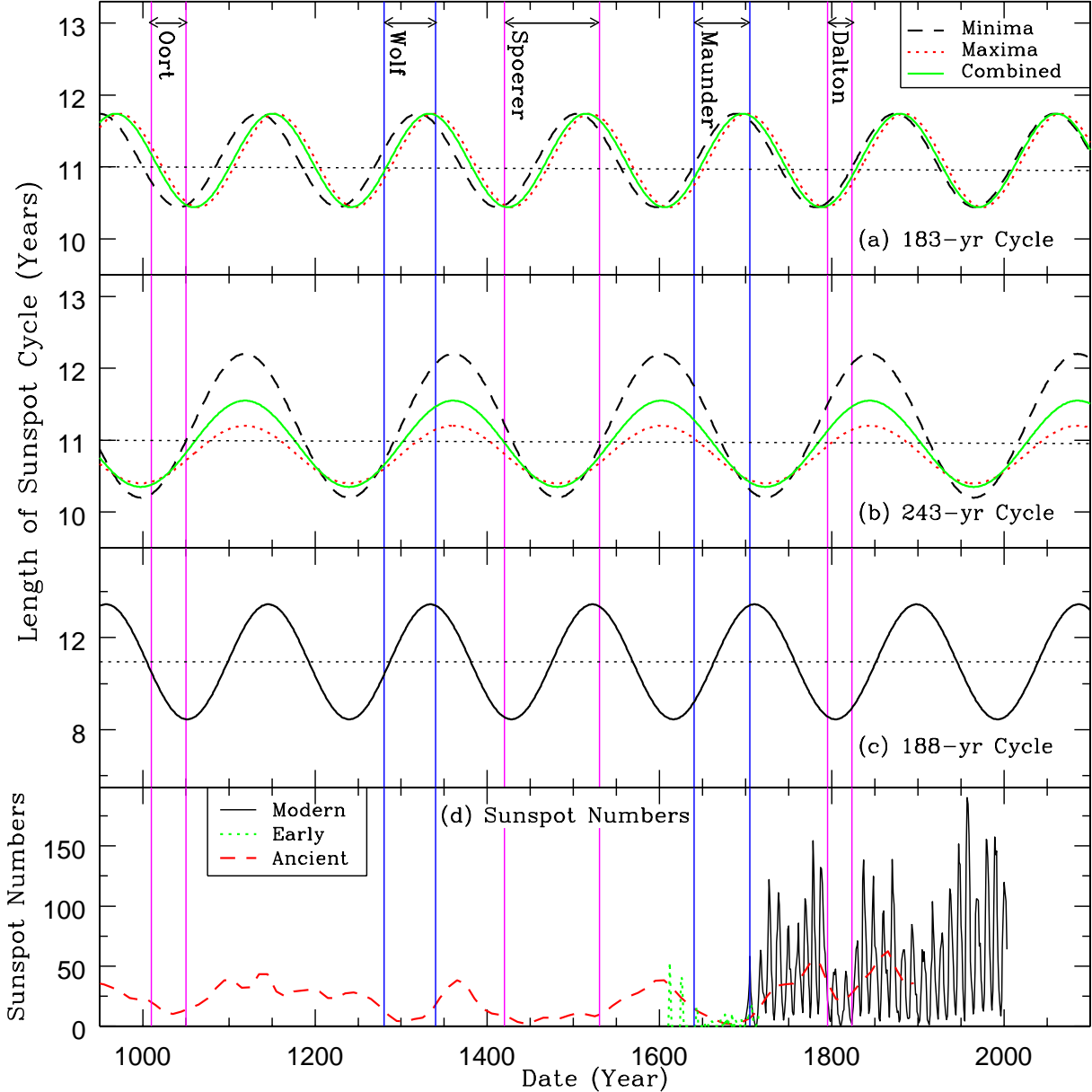


FIG. 8.— Sinusoidal fits to the sunspot number cycle corresponding to the derived periods of (a) 183 years, (b) 243 years, and (c) 188 years, compared with (d) the sunspot number data. The fits to (a) and (b) were produced from binned cycle minima (dashed line), cycle maxima (dotted line), and a combination of the two data sets (solid line). The bottom frame shows sunspot numbers from 1700 – 2004 (modern, solid line), 1610 – 1715 (early, dotted line), and 950 – 1950 (ancient, dashed line) reconstructed from radiocarbon data. The Dalton, Maunder, Spörer, Wolf, and Oort Minima are identified on the graph. The dates of these historical minima correspond well with the derived periodicities of 183 and 188 years, except for the Oort Minimum. The 243-year cycle does not match the historical minima as well as the other periodicities.